Articles

P−C Bond Cleavage of Phosphorus-Bridged [1]Ferrocenophane Coordinated to the [Cp(CO)₂Fe]⁺ Fragment

Tsutomu Mizuta,[†] Tomoaki Yamasaki,[†] Hiroshi Nakazawa,*,[†] and Katsuhiko Miyoshi*,[‡]

Coordination Chemistry Laboratories, Institute for Molecular Science, Myodaiji, Okazaki 444, Japan, and Department of Chemistry, Faculty of Science, Hiroshima University, Kagamiyama, Higashi-Hiroshima 739, Japan

An iron complex with (1,1′-ferrocenediyl)phenylphosphine (FCPP) as a ligand, [Cp(CO)₂Fe-(FCPP)]⁺, was prepared, and its PF₆⁻ salt was subjected to X-ray crystal structure analysis. Photoirradiation of the PF₆⁻ salt resulted in Cp ring migration from a P to an Fe atom. Addition of H₂O or (*n*-Bu)₄NF to the reaction mixture gave an isolable complex, formulated as [Cp(CO)Fe(C₅H₄FeC₅H₄PFPh)]. The structure for one of the racemic isomers was determined with X-ray analysis. This isomer was a kinetic product and isomerized to its thermodynamically stable epimer in the presence of an F⁻ anion.

Introduction

The ring-opening reaction of phosphorus-bridged [1]-ferrocenophane provides an important synthetic route to not only monomeric but also oligomeric and polymeric ferrocenylphosphine derivatives.[1,2] Most of the reactions involve P−C bond cleavage by RLi. Treatment of phosphorus-substituted lithioferrocenes thus prepared with a variety of electrophiles leads to 1,1′-disubstituted ferrocenes. Thermal ring-opening reactions have also been used[3,4] in some cases, though thermolysis has commonly been employed for the conversion of silicon-bridged [1]ferrocenophanes into polymeric silafer-rocenes.[5,6] The driving force of these ring-opening reactions comes from the ring strain present in a single-atom-bridged [1]ferrocenophane.[1a,d,7−11] Figure 1 shows a phosphorus-bridged [1]ferrocenophane. The two Cp rings are known to be considerably tilted (ca. 27°). Since the ferrocenophane has lone-pair electrons on the phosphorus, it may serve as a ligand toward a transition metal. Several complexes (**1−4**)[1b,12] possessing a phosphorus-bridged [1]ferrocenophane as a ligand have been synthesized. However, their reactivities have not yet been examined.
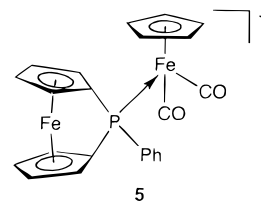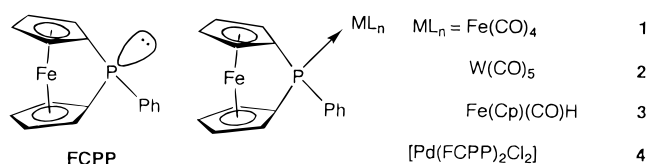
We are interested in the reactivity of a phosphorus-bridged [1]ferrocenophane coordinated to a transition metal. Since P−C bond activation by an organometallic

† Institute for Molecular Science.
‡ Hiroshima University.
⊗ Abstract published in *Advance ACS Abstracts,* January 1, 1996.
(1) (a) Seyferth, D.; Withers, H. P., Jr. *J. Organomet. Chem.* **1980,** *185,* C1. (b) Seyferth, D.; Withers, H. P., Jr. *Organometallics* **1982,** *1,* 1275. (c) Withers, H. P., Jr.; Seyferth, D.; Fellmann, J. D.; Garrou, P. E.; Martin, S. *Organometallics* **1982,** *1,* 1283. (d) Fellmann, J. D.; Garrou, P. E.; Withers, H. P., Jr.; Seyferth, D.; Traficante, D. D. *Organometallics* **1983,** *2,* 818.
(2) (a) Butler, I. R.; Cullen, W. R.; Einstein, F. W. B.; Rettig, S. J.; Willis, A. J. *Organometallics* **1983,** *2,* 128. (b) Butler, I. R.; Cullen, W. R. *Organometallics* **1984,** *3,* 1846. (c) Butler, I. R.; Cullen, W. R.; Einstein, F. W. B.; Willis, A. C. *Organometallics* **1985,** *4,* 603. (d) Butler, I. R.; Cullen, W. R. *Can. J. Chem.* **1983,** *61,* 147. (e) Butler, I. R.; Cullen, W. R. *Organometallics* **1986,** *5,* 2537.
(3) Cullen, W. R.; Rettig, S. J.; Zheng, T.-C. *J. Organomet. Chem.* **1993,** *452,* 97.
(4) Honeyman, C.; Foucher, D. A.; Mourad, O.; Rulkens, R.; Manners, I. *Polymer Prepr. (Am. Chem. Soc., Div. Polym. Chem.)* **1993,** *34* (1), 330.
(5) (a) Manners, I. *Adv. Organomet. Chem.* **1995,** *37,* 131. (b) Foucher, D.; Ziembinski, R.; Petersen, R.; Pudelski, J.; Edwards, M.; Ni, Y.; Massey, J.; Jaeger, C. R.; Vancso, G. J.; Manners, I. *Macromolecules* **1994,** *27,* 3992.
(6) (a) Nguyen, M. T.; Diaz, A. F.; Dement'ev, V. V.; Pannell, K. H. *Chem. Mater.* **1993,** *5,* 1389. (b) Nguyen, M. T.; Diaz, A. F.; Dement'ev, V. V.; Pannell, K. H. *Chem. Mater.* **1994,** *6,* 952.

(7) Stoeckli-Evans, H.; Osborne, A. G.; Whiteley, R. H. *Helv. Chim. Acta* **1976,** *59,* 2402.
(8) Butler, I. R.; Cullen, W. R.; Rettig, S. J. *Can. J. Chem.* **1987,** *65,* 1452.
(9) Finckh, W.; Tang, B.-Z.; Foucher, D. A.; Zamble, D. B.; Ziembinski, R.; Lough, A.; Manners, I. *Organometallics* **1993,** *12,* 823.
(10) Broussier, R.; Da Rold, A.; Gautheron, B.; Dromzee, Y.; Jeannin, Y. *Inorg. Chem.* **1990,** *29,* 1817.
(11) Stoeckli-Evans, H.; Osborne, A. G.; Whiteley, R. H. *J. Organomet. Chem.* **1980,** *194,* 91.
(12) Butler, I. R.; Cullen, W. R.; Rettig, S. J. *Organometallics* **1987,** *6,* 872.
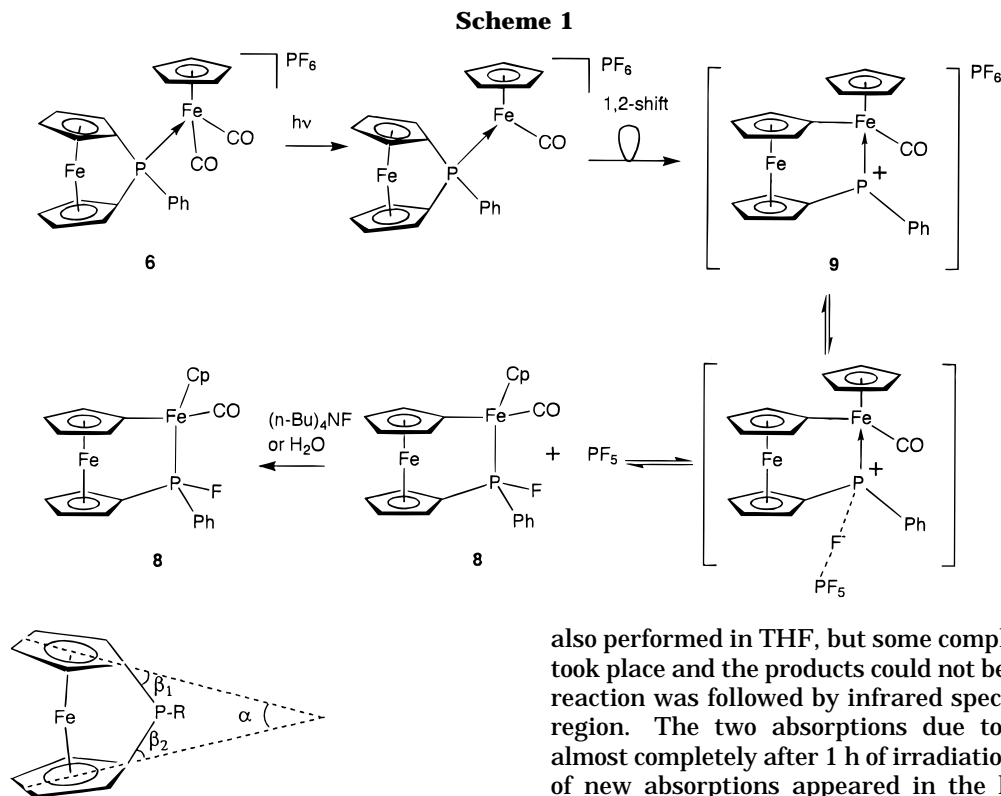
Scheme 1

Figure 1. Distortions in phosphorus-bridged [1]ferrocenophane, defining angles α and β.

complex is known,[13] it should be noteworthy to investigate what effect the coordination of the ferrocenophane exerts on its ring-opening reactivity (a P−C bond activation). We here focus on [Cp(CO)$_2$Fe(FCPP)]$^+$ (**5**), where (1,1′-ferrocenediyl)phenylphosphine (FCPP) coordinates through its phosphorus lone-pair electrons to a cationic [Cp(CO)$_2$Fe]$^+$ fragment, and report our findings that photochemical elimination of the carbonyl ligand promotes the ring-opening reaction, or 1,2-shift, of the Cp ring carbon from P to Fe with P−C bond activation.

Results and Discussion

Preparation of 6. The reaction of FCPP with [Cp-(CO)$_2$Fe(THF)]PF$_6$ in CH$_2$Cl$_2$ gave [Cp(CO)$_2$Fe(FCPP)]-PF$_6$ (**6**) in excellent yield. The infrared spectrum in the ν(CO) region showed two absorptions at 2056 and 2014 cm^{-1} in the CH$_2$Cl$_2$ solution, which are similar to those (2059 and 2016 cm^{-1}) for the PPh$_3$ analog [Cp(CO)$_2$Fe-(PPh$_3$)]PF$_6$ (**7a**).[14] The ^{31}P{^{1}H} NMR spectrum of **6** showed a singlet at 77.7 ppm, which is 64.4 ppm lower in magnetic field than that of free FCPP (13.3 ppm). A similar downfield shift has been observed for **7a** (−4.9 ppm for PPh$_3$ to 61.5 ppm).[15] The molecular structure of **6** was confirmed with X-ray analysis and is shown in Figure 2 (vide infra).

Photochemical Reaction of 6. **6** was irradiated with UV−vis light in CH$_2$Cl$_2$. (The photoreaction was

(13) Nakazawa, H.; Matsuoka, Y.; Nakagawa, I.; Miyoshi, K. *Organometallics* **1992**, *11*, 1385 and references therein.
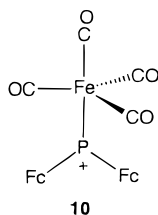(14) Literature values 2055 and 2010 cm^{-1}: (a) Treichel, P. M.; Shubkin, R. L.; Barnett, K. W.; Reichard, D. *Inorg. Chem.* **1966**, *5*, 1177. (b) Johnson, B. V.; Ouseph, P. J.; Hsieh, J. S.; Steinmetz, A. L.; Shade, J. E. *Inorg. Chem.* **1979**, *18*, 1796.
(15) Literature value of its BF$_4^-$ salt in 1,2-dichloroethane 67.9 ppm: Schumann, H.; Eguren, L. *J. Organomet. Chem.* **1991**, *403*, 183.

also performed in THF, but some complicated reactions took place and the products could not be identified.) The reaction was followed by infrared spectra in the ν(CO) region. The two absorptions due to **6** disappeared almost completely after 1 h of irradiation, and a number of new absorptions appeared in the lower frequency area. The ^{31}P{^{1}H} NMR spectrum of the reaction mixture also showed the complete disappearance of **6** and the appearance of new broad signals at over 200 ppm and under 50 ppm. Several attempts to isolate the products from the reaction mixture were unsuccessful. We, accordingly, tried to change the cationic species assumed to be formed into more stable species by addition of a nucleophile such as (*n*-Bu)$_4$NF or water. In both cases, the ^{31}P{^{1}H} NMR spectrum turned out to consist of four sharp signals above 200 ppm and a multiplet assigned to PF$_6^-$ as the major signals. Purification with an Al$_2$O$_3$ column led to the isolation of a red crystalline complex, **8**. Complex **8** was characterized as shown below by spectroscopic data. Since the complex has two chiral centers, Fe and P, it consists of the two diastereomeric pairs *RS*/*SR* (**8a**) and *RR*/*SS* (**8b**).
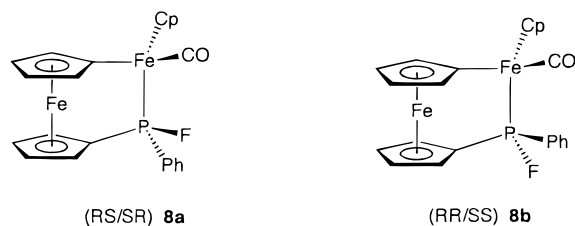
The intensities of the ^{31}P{^{1}H} NMR signals of the isolated complex **8** indicate that the four signals observed consist of two pairs of doublets at 220.8 and 242.5 ppm with the coupling constants 917.4 and 937.6 Hz, respectively. These large coupling constants are consistent with the presence of a P−F bond. The ^{19}F{^{1}H} NMR spectrum also supports the notion that **8** has a P−F bond: two doublets at −94.9 and −125.2 ppm with the coupling constants 937.6 and 918.0 Hz, respectively. The source of the fluorine atom in these reactions is discussed later.

The structure of **8** was determined by X-ray analysis. A red single crystal was obtained after repeated recrys-

tallization. Although the details of the structure will be mentioned later, it is pertinent to note here that the crystal obtained has an *RS/SR* configuration (**8a**). The $^{31}P\{^1H\}$ spectrum of **8a** showed one doublet at 220.8 ppm ($^1J_{P-F}$ = 917.4 Hz). Thus, the other doublet at 242.5 ppm ($^1J_{P-F}$ = 937.6 Hz) should be assigned to the other pair of diastereomers, *RR/SS* (**8b**).

Mechanism of Formation of [2]Ferrocenophane Complex 8 (8a,b). Let us consider the reaction mechanism for the transformation from **6** to **8**. The mechanism we propose is shown in Scheme 1. First, one CO ligand in **6** is activated by photolysis to generate a coodinatively unsaturated 16-e complex. Then, a Cp carbon in the FCPP fragment migrates from P to Fe (1,2-shift) to relieve the strain, yielding the phosphenium intermediate **9**. The phosphenium species produced may be a strong Lewis acid, and so the phosphenium phosphorus may interact with a PF_6^- anion through an F atom or abstract a fluoride from PF_6^-. Such an abstraction of a fluoride leaves PF_5, which is trapped when F^- or water is added.

Although the intermediate **9** could not be detected, this mechanism seems to be plausible for the following reasons. Photochemically induced loss of a CO followed by a 1,2-shift has been reported for the complex [Cp-$(CO)_2Fe-E^1R_2-E^2R'_3$] (E^1 and E^2 = Si and Ge) where the $E^2R'_3$ group migrates from the E^1 atom to the iron.[16,17] Since the phosphorus-bridged [1]ferrocenophane is highly strained as shown in Figure 2, where the Cp rings are tilted by 25.0° (vide infra), the phosphorus—Cp bond may be readily cleaved to become free from the strain. The 1,2-shift of the Cp to the iron yields the cationic phosphenium complex **9**. A ferrocene unit, abbreviated as Fc, has been utilized to stabilize a phosphenium.[18,19] For example, **10** was reported to be a stable phosphe-

10

nium complex, where the phosphenium phosphorus coordinates to an $Fe(CO)_4$ fragment and has two Fc

substituents.[19] In contrast, **9** is not stable enough to be detected, probably because the phosphenium phosphorus has one Fc and one Ph substituent. Since the latter substituent makes the Lewis acidity of the phosphenium phosphorus greater than that of **10**, because of the poor electron-donating ability of a Ph substituent compared with an Fc substituent, **9** may abstract a fluoride anion from PF_6^-. The abstraction of the fluoride by a metal-coordinated phosphenium has been proposed in a few reactions;[20,21] in eq 1, **11** reacts with
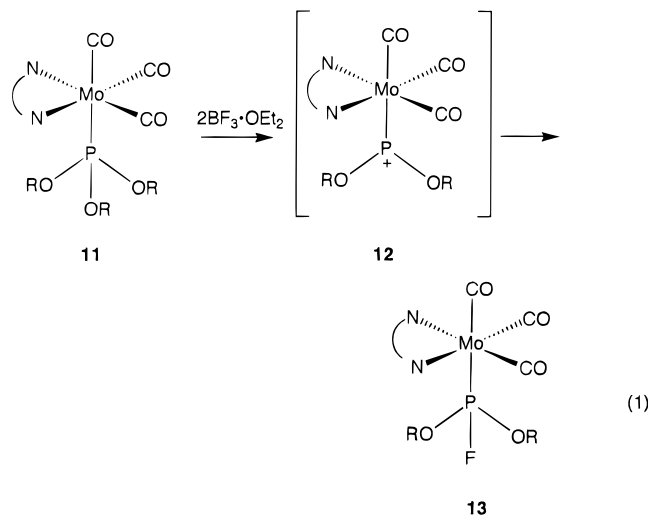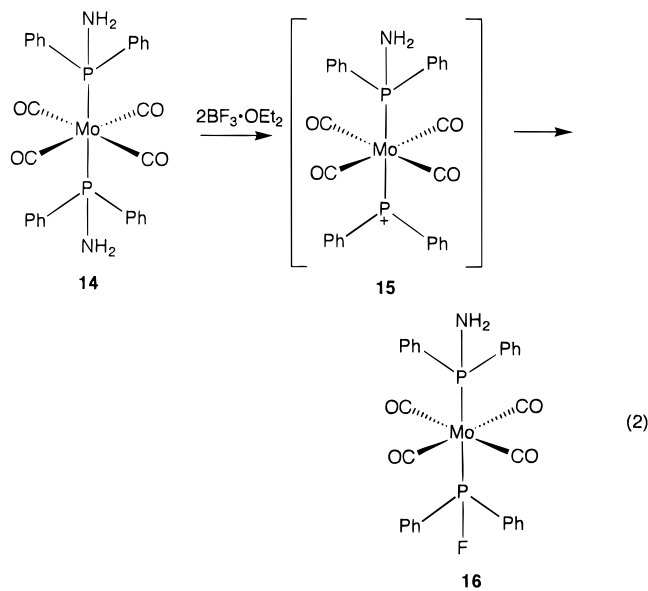
2 equiv of $BF_3 \cdot OEt_2$ to afford the mono OR/F exchange product **13**.[20] The reaction proceeds via the phosphenium intermediate **12**, which is not stable enough to be detected. In eq 2, the NH_2 of **14** is replaced by a fluorine. Though the authors mentioned nothing about the presence of the phosphenium species **15**,[21] it is highly plausible that the reaction proceeds via a phosphenium intermediate in analogy to eq 1. Since the

(16) (a) Tobita, H.; Ueno, K.; Ogino, H. *Chem. Lett.* **1986**, 1777. (b) Tobita, H.; Ueno, K.; Ogino, H. *Bull. Chem. Soc. Jpn.* **1988**, *61*, 2979. (c) Ueno, K.; Tobita, H.; Shimoi, M.; Ogino, H. *J. Am. Chem. Soc.* **1988**, *110*, 4092. (d) Tobita, H.; Ueno, K.; Shimoi, M.; Ogino, H. *J. Am. Chem. Soc.* **1990**, *112*, 3415. (e) Ueno, K.; Tobita, H.; Ogino, H. *Chem. Lett.* **1990**, 369. (f) Ueno, K.; Hamashima, N.; Shimoi, M.; Ogino, H. *Organometallics* **1991**, *10*, 959. (g) Koe, J. R.; Tobita, H.; Suzuki, T.; Ogino, H. *Organometallics* **1992**, *11*, 150. (h) Koe, J. R.; Tobita, H.; Ogino, H. *Organometallics* **1992**, *11*, 2479. (i) Takeuchi, T.; Tobita, H.; Ogino, H. *Organometallics* **1991**, *10*, 835. (j) Ueno, K.; Hamashima, N.;Ogino, H. *Organometallics* **1992**, *11*, 1435.
(17) (a) Pannell, K. H.; Cervantes, J.; Hernandez, C.; Cassias, J.; Vincenti, S. *Organometallics* **1986**, *5*, 1056. (b) Pannell, K. H.; Rozell, J. M.; Tsai, W.-M. *Organometallics* **1987**, *6*, 2085. (c) Pannell, K. H.; Rozell, J. M.; Hernandez, C. *J. Am. Chem. Soc.* **1989**, *111*, 4482. (d) Pannell, K. H.; Wang, L.-J.; Rozell, J. M. *Organometallics* **1989**, *8*, 550. (e) Pannell, K. H.; Sharma, S. *Organometallics* **1991**, *10*, 954. (f) Pannell, K. H.; Sharma, S. *Organometallics* **1991**, *10*, 1655. (g) Jones, K. L.; Pannell, K. H. *J. Am. Chem. Soc.* **1993**, *115*, 11336. (h) Hernandez, C.; Sharama, H. K.; Pannell, K. H. *J. Organomet. Chem.* **1993**, *462*, 259.
(18) Baxter, S. G.; Collins, R. L.; Cowley, A. H.; Sena, S. F. *J. Am. Chem. Soc.* **1981**, *103*, 715.
(19) Baxter, S. G.; Collins, R. L.; Cowley, A. H.; Sena, S. F. *Inorg. Chem.* **1983**, *22*, 3475.
(20) (a)Nakazawa, H.; Ohta, M.; Yoneda, H. *Inorg. Chem.* **1988**, *27*, 973. (b)Nakazawa, H.; Ohta, M.; Miyoshi, K.; Yoneda, H. *Organometallics* **1989**, *8*, 638.
(21) Bradley, F. C.; Wong, E. H.; Gabe, E. J.; Lee, F. L. *Inorg. Chim. Acta* **1986**, *120*, L21.

Table 1. Crystal and Refinement Data for Compounds 6 and 8a

	6	8a
(a) Crystal Data		
chem formula	$C_{23}H_{18}F_6Fe_2O_2P_2$	$C_{22}H_{18}FFe_2OP$
fw	614.03	460.05
cryst syst	orthorhombic	monoclinic
unit cell dimens		
a, Å	12.127(3)	29.534(4)
b, Å	14.530(2)	7.256(1)
c, Å	27.030(3)	20.029(2)
β, deg		120.943(9)
V, Å^3	4762(1)	3681.0(8)
space group	*Pbca* (No. 61)	*C2/c* (No. 15)
D_c, g cm^{-3}	1.713	1.660
Z	8	8
$F(000)$	2464.0	1872.0
color, habit	dark red, stick	red, plate
cryst dimens	$0.60 \times 0.42 \times 0.40$	$0.40 \times 0.33 \times 0.13$
μ, cm^{-1}	14.18	136.24
(b) Data Collection and Processing		
diffractometer	Enraf-Nonius CAD4	Enraf-Nonius CAD4
X-radiation	Mo Kα (graphite monochromated)	Cu Kα (graphite monochromated)
sacn mode	$\omega-\theta$	$\omega-\theta$
ω-scan width, deg	$0.80 + 0.35 \tan \theta$	$0.50 + 0.15 \tan \theta$
2θ limits, deg	60	140
data collected (*hkl*)	(002) to (17,20,38)	(−36,0,0) to (36,8,24)
no. of rflns		
total	7634	3869
unique (R_{int})	7634	3784 (0.112)
obsd	3630 ($I > 3\sigma(I)$)	2456 ($I > 3\sigma(I)$)
abs cor (transmissn factors)	DIFABS (0.6538−1.0763)	DIFABS (0.6580−1.7504)
(c) Structure Analysis and Refinement		
structure soln	direct methods (SAPI91)	direct methods (SAPI91)
refinement	full-matrix least squares	full-matrix least squares
no. of params	389	317
weighting scheme	$1/\sigma^2(F_0)$	$1/\sigma^2(F_0)$
R, %	0.054	0.049
R_w, %	0.051	0.047

phosphenium phosphorus in **15** is a strong Lewis acid because of the two Ph substituents, it abstracts the fluoride anion to give **16**. On the other hand, it was reported that a fluoride could be abstracted with PF$_5$ from a PF$_6^-$ anion.[22] If the acidity of **9** is much greater than that of PF$_5$, **9** abstracts the fluoride from its counteranion, PF$_6^-$, to leave the weaker Lewis acid PF$_5$ and the product **8**. Neither such a product nor the phosphenium species, however, could be observed in the ^{31}P{^{1}H} spectra after the irradiation. Therefore, we suppose that **9** and PF$_5$ are comparable in acidity and/ or that the reaction from **9** to the products is a fast equilibrium. Once water is added to this equilibrium, PF$_5$ is immediately trapped to produce **8**.

The reaction in Scheme 1 involves P−C bond activation by a transition-metal complex. Recently, many results concerning P−C bond activation have been reported,[13] and some of the P−C activations have been proposed to be attained by migration of an alkyl or an aryl group in a phosphorus compound coordinated to a transition metal to its transition metal. Although clear evidence for this type of migration has not been given in these reports, our present results afford unambiguous evidence.

Isomerization Reaction between 8a and 8b. It is noteworthy that the ratio of **8a** to **8b** is dependent on the kind of additive. When (*n*-Bu)$_4$NF was used as an additive, the ratio was 1:5, whereas when water was used, the ratio was 3:1. To elucidate the reason for this difference, the isomerization between the diastereomers

8a and **8b** was examined. **8a** isolated by recrystallization was dissolved in CH$_2$Cl$_2$ at room temperature, and the isomerization was monitored in the ^{31}P{^{1}H} spectra. No reaction, however, was observed after 24 h. Then, the same treatment was done in the presence of 1 equiv of (*n*-Bu)$_4$NF. The NMR intensity of the starting diastereomer **8a** decreased within 3 min to reach the ratio of 1:5 for **8a**:**8b**, which means that **8b** is thermodynamically more stable than **8a**. This is reasonable from the viewpoint of steric hindrance between the Cp and the Ph groups on the two asymmetric centers. The two bulky Cp and Ph groups on Fe(2) and P(1), respectively, take a pseudo-eclipsed configuration in **8a** as shown in Figure 3, whereas they take a pseudo-gauche configuration in **8b**. Since the isomerization is accelerated drastically in the presence of F$^-$, it proceeds via the associative mechanism as shown in the bottom path of Scheme 2, where F$^-$ attacks the phosphorus atom from the opposite side of the P−F bond to form a five-coordinate species as an intermediate; nucleophilic attack of a nucleophile such as F$^-$, H$^-$, or $^-$OR to a coordinating trivalent phosphorus has been reported to give metallaphosphorane.[23,24]

In the reaction shown in Scheme 1, **8a** is dominantly produced as a kinetic product, whereas in the presence of excess F$^-$, i.e. (*n*-Bu)$_4$NF, **8a** is converted into the thermodynamic product **8b**. Such a kinetic effect is part of the evidence for the phosphenium intermediate as

(22) Brownstein, S.; Bornais, J. *Can. J. Chem.* **1968**, *46*, 225.

(23) Mason, M. R.; Verkade, J. G. *Organometallics* **1992**, *11*, 2212.
(24) (a) Nakazawa, H.; Kubo, K.; Kai, C.; Miyoshi, K. *J. Organomet. Chem.* **1992**, *439*, C42. (b) Nakazawa, H.; Kubo, K.; Miyoshi, K. *J. Am. Chem. Soc.* **1993**, *115*, 5863.

Scheme 2
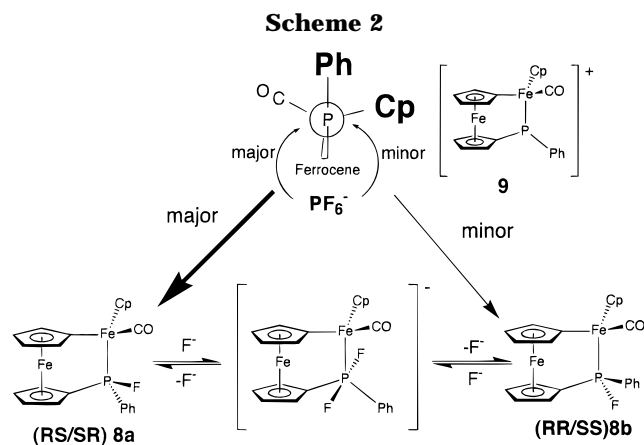
Table 2. Final Fractional Coordinates and Thermal Parameters for the Non-Hydrogen Atoms of 6

atom	x	y	z	B_{eq},[a] Å^2
Fe(1)	0.12865(6)	0.24833(6)	0.99230(3)	4.88(2)
Fe(2)	0.04493(6)	0.14101(5)	0.84207(3)	3.59(2)
P(1)	0.1615(1)	0.18209(9)	0.90043(5)	3.47(3)
P(2)	0.2396(1)	0.4187(1)	0.69581(7)	5.47(4)
F(1)	0.1449(5)	0.4234(4)	0.7329(2)	16.1(2)
F(2)	0.2432(4)	0.5258(2)	0.6965(2)	10.4(1)
F(3)	0.1525(4)	0.4269(3)	0.6537(2)	12.3(2)
F(4)	0.3261(5)	0.4111(4)	0.7356(2)	16.6(2)
F(5)	0.2339(4)	0.3120(3)	0.6941(2)	12.1(2)
F(6)	0.3315(4)	0.4110(4)	0.6567(2)	13.0(2)
O(1)	−0.1594(3)	0.1561(4)	0.8976(2)	8.2(1)
O(2)	0.0913(4)	−0.0492(3)	0.8650(2)	8.5(2)
C(1)	0.1500(4)	0.3002(3)	0.9248(2)	4.4(1)
C(2)	0.0446(4)	0.3286(4)	0.9442(2)	5.0(1)
C(3)	0.0630(5)	0.3806(4)	0.9876(3)	6.2(2)
C(4)	0.1773(6)	0.3859(4)	0.9966(3)	6.4(2)
C(5)	0.2311(5)	0.3370(4)	0.9585(2)	5.3(2)
C(6)	0.1496(5)	0.1262(3)	0.9611(2)	4.5(1)
C(7)	0.0458(6)	0.1280(4)	0.9872(2)	5.4(2)
C(8)	0.0680(6)	0.1443(5)	1.0375(2)	6.9(2)
C(9)	0.1814(7)	0.1518(6)	1.0444(2)	7.3(2)
C(10)	0.2326(6)	0.1408(5)	0.9978(2)	5.8(2)
C(11)	0.3046(4)	0.1646(3)	0.8843(2)	3.9(1)
C(12)	0.3674(5)	0.2349(4)	0.8644(2)	5.1(2)
C(13)	0.4762(6)	0.2203(6)	0.8513(3)	6.3(2)
C(14)	0.5222(6)	0.1354(7)	0.8573(3)	7.0(2)
C(15)	0.4617(6)	0.0645(5)	0.8770(3)	6.6(2)
C(16)	0.3519(5)	0.0781(4)	0.8903(2)	5.0(2)
C(17)	0.0135(7)	0.2535(6)	0.7963(3)	6.8(2)
C(18)	−0.0456(7)	0.1771(7)	0.7799(3)	6.9(2)
C(19)	0.0291(10)	0.1098(7)	0.7678(2)	7.7(3)
C(20)	0.1359(7)	0.1436(6)	0.7768(2)	6.3(2)
C(21)	0.1237(6)	0.2321(5)	0.7939(2)	5.7(2)
C(22)	−0.0778(5)	0.1502(4)	0.8773(2)	5.3(1)
C(23)	0.0721(5)	0.0247(4)	0.8561(2)	5.0(1)

[a] $B_{eq} = \frac{8}{3}\pi^2(U_{11}(aa^*)^2 + U_{22}(bb^*)^2 + U_{33}(cc^*)^2 + 2U_{12}aa^*bb^* \cos\gamma + 2U_{13}aa^*cc^* \cos\beta + 2U_{23}bb^*cc^* \cos\alpha)$.

shown at the top of Scheme 2. When PF_6^- attacks the phosphenium phosphorus, which has a trigonal-planar geometry, the approach from the CO side may be preferable to that from the bulky Cp side, making **8a** the major kinetic product.

X-ray Structures of 6 and 8a. Single crystals of **6** and **8a** were obtained from CH_2Cl_2/Et_2O. The cell constants and the data collection parameters are summarized in Table 1. The fractional coordinates and important bond lengths and angles are listed in Tables 2−5.

In **6,** shown in Figure 2, the Fe(2)−P(1) distance (2.201(2) Å) is slightly shorter than that (2.242(1) Å) in

Table 3. Selected Bond Lengths (Å) and Angles (deg) for 6 with Estimated Standard Deviations in Parentheses

Lengths			
Fe(1)−C(1)	1.992(5)	Fe(1)−C(2)	2.022(6)
Fe(1)−C(3)	2.084(7)	Fe(1)−C(4)	2.088(7)
Fe(1)−C(5)	2.009(6)	Fe(1)−C(6)	1.981(5)
Fe(1)−C(7)	2.021(7)	Fe(1)−C(8)	2.078(7)
Fe(1)−C(9)	2.087(7)	Fe(1)−C(10)	2.014(7)
Fe(2)−P(1)	2.201(2)	Fe(2)−C(22)	1.773(6)
Fe(2)−C(23)	1.763(6)	P(1)−C(1)	1.844(5)
P(1)−C(6)	1.837(5)	P(1)−C(11)	1.807(5)
O(1)−C(22)	1.134(6)	O(2)−C(23)	1.125(6)
C(1)−C(2)	1.442(7)	C(1)−C(5)	1.444(8)
C(2)−C(3)	1.412(8)	C(3)−C(4)	1.409(9)
C(4)−C(5)	1.411(8)	C(6)−C(7)	1.444(7)
C(6)−C(10)	1.428(8)	C(7)−C(8)	1.405(8)
C(8)−C(9)	1.39(1)	C(9)−C(10)	1.413(9)

Angles			
P(1)−Fe(2)−C(22)	97.7(2)	P(1)−Fe(2)−C(23)	89.2(2)
C(22)−Fe(2)−C(23)	96.5(3)	Fe(2)−P(1)−C(1)	117.3(2)
Fe(2)−P(1)−C(6)	118.0(2)	Fe(2)−P(1)−C(11)	114.0(2)
C(1)−P(1)−C(6)	95.0(2)	C(1)−P(1)−C(11)	106.8(2)
C(6)−P(1)−C(11)	103.2(2)	P(1)−C(1)−C(2)	117.6(4)
P(1)−C(1)−C(5)	121.2(4)	C(2)−C(1)−C(5)	105.5(5)
C(1)−C(2)−C(3)	108.4(6)	C(2)−C(3)−C(4)	109.1(6)
C(3)−C(4)−C(5)	107.6(6)	C(1)−C(5)−C(4)	109.4(6)
P(1)−C(6)−C(7)	119.8(4)	P(1)−C(6)−C(10)	119.9(4)
C(7)−C(6)−C(10)	105.9(5)	C(6)−C(7)−C(8)	107.9(6)
C(7)−C(8)−C(9)	109.4(6)	C(8)−C(9)−C(10)	107.9(6)
C(6)−C(10)−C(9)	108.9(6)	Fe(2)−C(22)−O(1)	176.4(5)
Fe(2)−C(23)−O(2)	178.8(6)		

Table 4. Final Fractional Coordinates and Thermal Parameters for the Non-Hydrogen Atoms of 8a

atom	x	y	z	B_{eq},[a] Å^2
Fe(1)	0.69338(3)	0.1929(1)	0.31384(5)	1.77(2)
Fe(2)	0.55770(3)	0.1826(1)	0.17131(5)	2.24(2)
P(1)	0.61431(6)	0.0618(2)	0.14673(8)	2.23(3)
F(1)	0.5970(1)	−0.1434(5)	0.1112(2)	3.40(9)
O(1)	0.5591(2)	−0.1484(7)	0.2530(3)	5.1(1)
C(1)	0.6183(2)	0.2974(8)	0.2644(3)	1.8(1)
C(2)	0.6388(3)	0.2457(9)	0.3449(4)	2.5(1)
C(3)	0.6860(3)	0.3472(10)	0.3936(4)	2.9(2)
C(4)	0.6968(3)	0.4614(9)	0.3463(4)	3.0(2)
C(5)	0.6547(2)	0.4311(9)	0.2681(4)	2.5(1)
C(6)	0.6788(2)	0.0154(8)	0.2286(3)	2.1(1)
C(7)	0.6891(3)	−0.0815(9)	0.2982(3)	2.5(1)
C(8)	0.7408(2)	−0.0385(10)	0.3580(4)	2.7(1)
C(9)	0.7626(2)	0.0876(10)	0.3277(4)	2.9(2)
C(10)	0.7249(2)	0.1235(10)	0.2478(4)	2.5(1)
C(11)	0.6284(2)	0.1501(9)	0.0756(3)	2.3(1)
C(12)	0.6559(3)	0.0444(10)	0.0504(4)	3.0(2)
C(13)	0.6645(3)	0.0992(12)	−0.0081(4)	3.9(2)
C(14)	0.6462(3)	0.2668(14)	−0.0418(4)	4.6(2)
C(15)	0.6211(3)	0.3831(14)	−0.0168(5)	4.6(2)
C(16)	0.6122(2)	0.3256(11)	0.0422(4)	3.4(2)
C(17)	0.5260(3)	0.4243(12)	0.1062(4)	3.7(2)
C(18)	0.5113(3)	0.4086(14)	0.1619(5)	4.3(2)
C(19)	0.4822(2)	0.2496(12)	0.1513(4)	3.9(2)
C(20)	0.4771(3)	0.1641(15)	0.0844(4)	5.0(2)
C(21)	0.5039(3)	0.2691(13)	0.0577(4)	4.2(2)
C(22)	0.5600(2)	−0.0158(9)	0.2209(4)	3.0(2)

[a] See footnote *a* in Table 2.

$[Cp(CO)_2Fe(PPh_3)]Cl \cdot 3H_2O$ (**7b**)[25] and that (2.240(1) Å) in $[Cp(CO)_2Fe(PPh_3)]\{(NC)_2CC(CN)C(CN)_2\}$ (**7c**; $(NC)_2$-$CC(CN)C(CN)_2 = 1,1,2,3,3$-pentacyanopropenide).[26] The Fe−CO distances (1.773(5) and 1.763(6) Å) are almost the same as those in **7b,c** (1.775(4) and 1.767(4) Å, and 1.778(5) and 1.774(7) Å, respectively), as expected from

(25) Riley, P. E.; Davis, R. E. *Organometallics* **1983**, *2*, 286.
(26) Sim, G. A.; Woodhouse, D. I.; Knox, G. R. *J. Chem. Soc., Dalton Trans.* **1979**, 629.
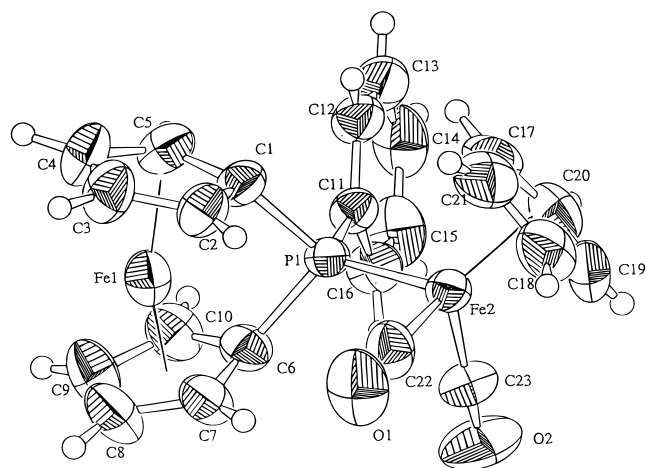
Figure 2. Crystal structure of $[Cp(CO)_2Fe(FCPP)]^+$ in **6** with the numbering scheme. Thermal ellipsoids are drawn at 50% probability. PF_6^- was eliminated for clarity.

Table 5. Selected Bond Lengths (Å) and Angles (deg) for 8a with Estimated Standard Deviations in Parentheses

Lengths			
Fe(1)−C(1)	2.053(5)	Fe(1)−C(2)	2.039(6)
Fe(1)−C(3)	2.051(6)	Fe(1)−C(4)	2.039(7)
Fe(1)−C(5)	2.014(7)	Fe(1)−C(6)	2.001(6)
Fe(1)−C(7)	2.009(6)	Fe(1)−C(8)	2.072(6)
Fe(1)−C(9)	2.063(6)	Fe(1)−C(10)	2.035(6)
Fe(2)−P(1)	2.157(2)	Fe(2)−C(1)	1.985(5)
Fe(2)−C(22)	1.730(7)	P(1)−F(1)	1.616(4)
P(1)−C(6)	1.795(6)	P(1)−C(11)	1.796(6)
O(1)−C(22)	1.165(7)	C(1)−C(2)	1.449(7)
C(1)−C(5)	1.422(8)	C(2)−C(3)	1.427(9)
C(3)−C(4)	1.412(9)	C(4)−C(5)	1.429(8)
C(6)−C(7)	1.446(7)	C(6)−C(10)	1.442(8)
C(7)−C(8)	1.408(8)	C(8)−C(9)	1.422(9)
C(9)−C(10)	1.427(8)		

Angles			
P(1)−Fe(2)−C(1)	87.4(2)	P(1)−Fe(2)−C(22)	89.2(2)
C(1)−Fe(2)−C(22)	93.4(3)	Fe(2)−P(1)−F(1)	111.6(1)
Fe(2)−P(1)−C(6)	116.8(2)	Fe(2)−P(1)−C(11)	124.0(2)
F(1)−P(1)−C(6)	100.2(2)	F(1)−P(1)−C(11)	97.4(2)
C(6)−P(1)−C(11)	102.8(3)	Fe(2)−C(1)−C(2)	126.5(5)
Fe(2)−C(1)−C(5)	128.9(4)	C(2)−C(1)−C(5)	104.2(5)
C(1)−C(2)−C(3)	109.3(6)	C(2)−C(3)−C(4)	108.8(6)
C(3)−C(4)−C(5)	106.0(6)	C(1)−C(5)−C(4)	111.7(6)
Fe(1)−C(6)−P(1)	108.6(3)	P(1)−C(6)−C(7)	124.7(4)
P(1)−C(6)−C(10)	123.7(5)	C(7)−C(6)−C(10)	107.8(5)
C(6)−C(7)−C(8)	108.2(6)	C(7)−C(8)−C(9)	108.0(6)
C(8)−C(9)−C(10)	109.5(6)	C(6)−C(10)−C(9)	106.5(6)
Fe(2)−C(22)−O(1)	176.9(6)		

the ν(CO) frequencies of **6** and **7a**. These structural and spectroscopic similarities between $[Cp(CO)_2Fe(FCPP)]^+$ and $[Cp(CO)_2Fe(PPh_3)]^+$ indicate that FCPP serves as a donor ligand similarly to PPh_3.

As shown in Figure 2 and Table 6, the two Cp rings in the [1]ferrocenophane unit in **6** are considerably tilted as expected. The dihedral angle, α, is 25.0°, which is comparable to the value of 26.9° for the free ligand FCPP.[2a] It is thus confirmed that the strain of the [1]-ferrocenophane unit is almost intact when FCPP coordinates to a metal, as previously described for [Cp(CO)-HFe(FCPP)] (**3**), in which α is 25.4°.[12] The structural differences among FCPP, [Cp(CO)HFe(FCPP)] (**3**), and $[Cp(CO)_2Fe(FCPP)]PF_6$ (**6**) in Table 6 give us an interesting structural feature of the phosphorus-bridged [1]-ferrocenophane. The distances between the bridging phosphorus atom and the iron atom in the ferrocene unit are 2.774(2), 2.731(2), and 2.693(2) Å for free FCPP, **3**,

Table 6. Selected Structural Data for (1,1'-Ferrocenediyl)phenylphosphine (FCPP) and Iron Complexes with FCPP as a Ligand

	FCPP (free ligand)	[CpH(CO)-Fe(FCPP)] (**3**)	[Cp(CO)$_2$Fe-(FCPP)]PF$_6$ (**6**)
P−Fe,[a] Å	2.774(1)	2.731(2)	2.693(2)
P−C(Cp), Å	1.849(5)	1.837(6)	1.837(5)
	1.850(5)	1.841(5)	1.844(5)
ring tilt, α, deg	26.9	25.4	25.0
β,[b] deg	32.3	33.9	34.6
ref	2a	12	this work

[a] Distance between the bridging phosphorus atom and the iron atom of the ferrocene unit. [b] Average of the angles β_1 and β_2 in Figure 1.
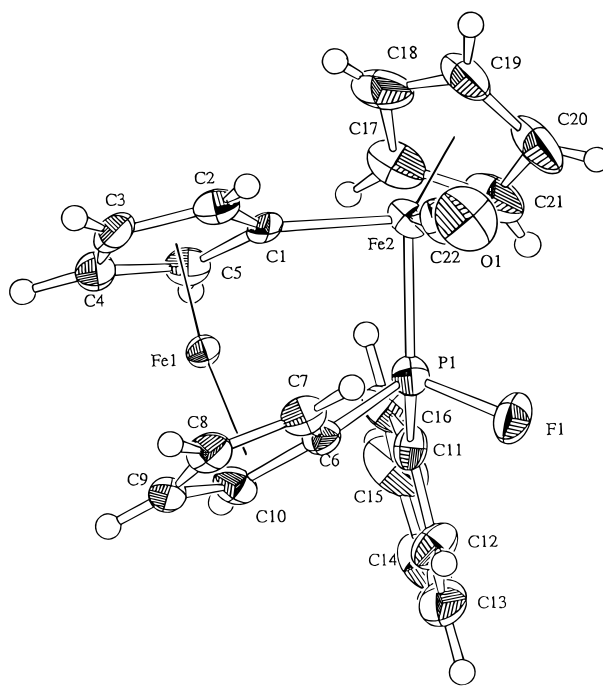

Figure 3. Molecular structure of **8a** with the numbering scheme. Thermal ellipsoids are drawn at 50% probability.

and **6**, respectively, indicating that the phosphorus atom slightly approaches the iron atom in this order. The shortening of the P−Fe(ferrocene) distance causes a decrease of the tilt angle α and an increase of β, because the bridging P−C (in Cp) bond distances are almost constant. The reason for this shortening may come from a weak interaction between the phosphorus atom and the iron atom. Silver proposed, for some [1]ferro-cenophanes on the basis of the Mössbauer data, a weak interaction between a vacant d orbital of the bridging phosphorus and a filled d orbital of the iron, though the distance between them is considerably longer than that of the normal Fe−P bonds.[27] In the series of phosphorus-bridged [1]ferrocenophanes in Table 6, the lone-pair electrons of the phosphine are withdrawn more by the cationic dicarbonyl fragment $[Cp(CO)_2Fe]^+$ than by the neutral monocarbonyl fragment [Cp(CO)HFe]. Thus, the phosphorus atom in $[Cp(CO)_2Fe(FCPP)]^+$ becomes the most electron-deficient and may interact most strongly with the iron atom. As a result, the phosphorus atom is closer to the iron in the order free FCPP, [Cp-(CO)HFe(FCPP)], and $[Cp(CO)_2Fe(FCPP)]PF_6$. Similar structural deformation was observed for a series of

(27) Houlton, A.; Roberts, R. M. G.; Silver, J.; Drew, M. G. B. *J. Chem. Soc., Dalton Trans.* **1990**, 1543.
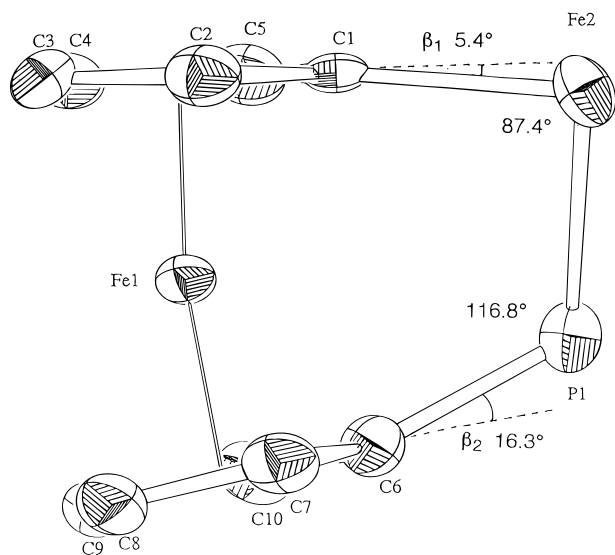
Figure 4. Distortions in the [2]ferrocenophane unit of **8a**. β_1 and β_2 are the angles defined by the least-squares plane of the C_5 ring and C(1)−Fe(2) bond or C(6)−P(1) bond, respectively.

silicon-bridged [1]ferrocenophanes, $(R'C_5H_3FeC_5H_4)SiR_2$ (R = Me, R' = H; R = Ph, R' = H; R = Cl, R' = CH-(Me)NMe₂), in which the distance between the silicon and iron atom[9] (2.690(3), 2.636(5), and 2.5931(1) Å for R = Me,[9] Ph,[7] Cl,[8] respectively) decreases depending on the electronegativity of R.

In **8a**, shown in Figure 3, the ferrocene unit is bridged by the Fe(2)−P(1) group. Fe(2) is surrounded by η^5-Cp, CO, η^1-Cp, and the phosphorus ligand to make the well-known piano-stool type geometry. Fe(2), Ph, η^1-Cp, and F(1) bond to P(1) to make a tetrahedral geometry. The structure in Figure 4 shows a heteroatom-bridged [2]-ferrocenophane unit. This unit is similar to that of the previously reported **17**,[2b] corresponding to a complex formally formed by a replacement of F in **8a** by Ph. The tilt angles of the ferrocene unit are 11.7 and 11.5° for **8a** and **17**, respectively. Though these angles are significantly reduced from the tilt angle of the parent [1]ferrocenophane (for example, 25.0° for **6**), their values mean that the Fe−P bonds (2.157(2) and 2.116(5) Å for **8a** and **17**, respectively) are still short as a bridging part of a strain-free ferrocene. Further reduction of the tilt angle was observed for **18**, in which α is 4.2° and the Si−Si distance is 2.3535(9) Å.[9,28]

17   **18**
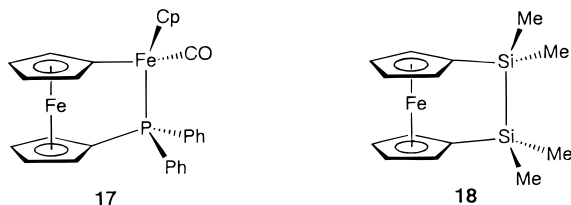
Other distortion parameters, β_1 and β_2, reflect the properties of the bridging atoms, as shown in Figure 4. β_1's for **8a** and **17** are 5.4 and 5.2°, respectively, whereas β_2's are 16.3 and 13.1°, respectively. A piano-stool type of transition-metal complex prefers a right angle for the bond angles between the three legs, whereas a phosphorus atom tends to take a tetrahedral angle. Actu-

ally, the C_5H_4−Fe−P bond angles are 87.4(2) and 90.46(5)°, and the C_5H_4−P−Fe bond angles are 116.8-(2) and 114.08(5)° for **8a** and **17**, respectively. As a result, the bridging Fe−P group shifts slightly from the symmetrical position to the upper side to enjoy the preferred angle for each atom, making β_1 considerably smaller than β_2.

Experimental Section

General Remarks. All reactions were carried out under an atmosphere of dry nitrogen using Schlenk tube techniques. CH_2Cl_2 and ether were distilled from P_2O_5 and sodium metal, respectively, and stored under an nitrogen atmosphere.

IR spectra were recorded on a Shimadzu FTIR-8100A spectrometer. JEOL EX-270, EX-400, and LA-500 spectrometers were used to obtain ¹H, ¹³C, ¹⁹F, and ³¹P NMR spectra. ¹H and ¹³C NMR data were referenced to $(CH_3)_4Si$, ¹⁹F NMR data to $CFCl_3$, and ³¹P NMR data to 85% H_3PO_4. A Shimadzu GCMS QP-1000EX was used to obtain mass spectra.

Preparation of 6. **6** was prepared from $[Cp(CO)_2Fe(THF)]$-PF_6 and FCPP in a manner similar to that for $[Cp(CO)_2Fe$-$\{P(OMe)_3\}]PF_6$.[29,30]

$[Cp(CO)_2Fe(THF)]PF_6$ (1.43 g, 3.62 mmol) and FCPP (1.06 g, 3.63 mmol) were treated in 30 mL of CH_2Cl_2 at room temperature. After the mixture was stirred for over 30 min, removal of the solvent under reduced pressure yielded a brown residue. After this was crushed into powder, it was washed twice with 20 mL of ether and then dried in vacuo to give **6** (2.20 g, 3.58 mmol, 95%). ¹H NMR (270 MHz, CDCl₃): δ 4.42, 4.64, 4.78, and 4.94 (m, 8H, ferrocene), 5.25 (s, 5H, Cp), 7.57−7.85 (m, 5H, Ph). ¹³C{¹H} NMR (CD₃COCD₃): δ 19.3 (d, ¹$J_{C−P}$ = 27.5 Hz, ferrocene), 77.0 (d, $J_{C−P}$ = 18.6 Hz, ferrocene), 77.7 (d, $J_{C−P}$ = 3.4 Hz, ferrocene), 81.6 (d, $J_{C−P}$ = 11.7 Hz, ferrocene), 81.6 (d, $J_{C−P}$ = 3.4 Hz, ferrocene), 89.9 (s, Cp), 130.3 (d, $J_{C−P}$ = 10.3 Hz, Ph), 131.0 (d, $J_{C−P}$ = 11.7 Hz, Ph), 133.5 (d, ¹$J_{C−P}$ = 55.7 Hz, P-ipso-Ph), 133.6 (d, $J_{C−P}$ = 3.4 Hz, Ph), 220.8 (d, ²$J_{C−P}$ = 24.7 Hz, CO). ³¹P{¹H} NMR (CH_2Cl_2): δ 77.7. IR (ν(CO), CH_2Cl_2 solution): 2056, 2014 cm⁻¹. Anal. Calcd for $C_{23}H_{18}F_6Fe_2O_2P_2$: C, 44.99; H, 2.95. Found: C, 45.23; H, 3.17.

Photoreaction of 6 and Isolation of the Product 8. A Pyrex Schlenk tube connected to a vent was charged with **6** (648 mg, 1.06 mmol) dissolved in 20 mL of CH_2Cl_2. Irradiation was carried out in an ice-cooled bath with a 400 W medium-pressure Hg arc lamp for 1 h. Then, 2 mL of water was added to the solution. After it was stirred for a few minutes, the solution was loaded on an Al_2O_3 column. An orange band eluted with CH_2Cl_2 was collected. After removal of the solvent, the residue was dried in vacuo to give a mixture of **8a** and **8b** (100 mg, 0.237 mmol, 22%). Anal. Calcd for $C_{22}H_{18}FFe_2OP$: C, 57.44; H, 3.94. Found: C, 57.33; H, 4.10.

The diastereomeric mixture thus obtained was recrystallized several times by addition of ether to the CH_2Cl_2 solution. The crystals obtained were **8a**. Spectroscopic data for **8a** are as follows. ¹H NMR (270 MHz, CDCl₃): δ 3.88, 3.92, 4.11, 4.28, 4.36, 4.47, and 5.25 (m, 8H, ferrocene), 4.55 (d, ³$J_{H−P}$ = 1.3 Hz, 5H, Cp), 7.58−8.02 (m, 5H, Ph). ¹³C{¹H} NMR (CDCl₃): δ 65.7 (d, J = 24.2 Hz, ferrocene), 68.8 (d, J = 8.1 Hz, ferrocene), 72.0 (d, J = 2.7 Hz, ferrocene), 72.7 (d, J = 29.6 Hz, ferrocene), 72.8 (d, J = 32.3 Hz, ferrocene), 73.2 (d, J = 12.1 Hz, ferrocene), 74.4 (s, ferrocene), 82.3 (s, ferrocene), 83.1 (s, Cp), 83.9 (s, ferrocene), 86.7 (dd, J = 33.6 and 63.2 Hz, P-ipso-ferrocene), 128.5 (d, J = 10.7 Hz, Ph), 129.6 (dd, J = 4.8 and 12.1 Hz, Ph), 131.0 (s, Ph), 139.1 (dd, J = 13.4 and 29.6 Hz, P-ipso-Ph), 221.3 (dd, J = 4.0 and 43.1 Hz, CO). ¹⁹F{¹H} NMR (CH_2Cl_2): δ −94.39 (d, ¹$J_{F−P}$ = 918.0 Hz).

(28) Dement'ev, V. V.; Cervantes-Lee, F.; Parkanyi, L.; Sharma, H.; Pannell, K. H.; Nguyen, M. T.; Diaz, A. *Organometallics* **1993**, *12*, 1983.

(29) Catheline, D.; Astruc, D. *Organometallics* **1984**, *3*, 1094.
(30) Nakazawa, H.; Kubo, K.; Tanisaki, K.; Kawamura, K.; Miyoshi, K. *Inorg. Chim. Acta* **1994**, *222*, 123.

^{31}P{^{1}H} NMR (CH$_2$Cl$_2$): δ 220.8 (d, $^1J_{P-F}$ = 917.4 Hz). IR (ν(CO), CH$_2$Cl$_2$ solution): 1936 cm^{-1}.

Spectroscopic data for **8b** are as follows. ^{1}H NMR (270 MHz, CDCl$_3$): δ 4.10, 4.18, 4.28, 4.41, 4.46, 4.50, and 5.00 (m, 8H, ferrocene), 4.71 (d, $^3J_{H-P}$ = 1.0 Hz, 5H, Cp), 7.45–7.79 (m, 5H, Ph). ^{13}C{^{1}H} NMR (CDCl$_3$): δ 68.7 (d, J = 7.4 Hz, ferrocene), 70.1 (d, J = 17.0 Hz, ferrocene), 70.1 (d, J = 23.2 Hz, ferrocene), 71.5 (d, J = 2.5 Hz, ferrocene), 72.3 (d, J = 9.8 Hz, ferrocene), 73.3 (d, J = 9.7 Hz, ferrocene), 74.0 (s, ferrocene), 82.0 (s, ferrocene), 83.0 (s, ferrocene), 83.1 (s, Cp), 87.1 (dd, J = 17.0 and 42.8 Hz, P-ipso-ferrocene), 128.4 (d, J = 9.7 Hz, Ph), 130.2 (d, J = 14.6 Hz, Ph), 131.5 (s, Ph), 142.7 (dd, J = 14.6 and 34.1 Hz, P-ipso-Ph), 220.9 (dd, J = 4.9 and 31.7 Hz, *C*O). ^{19}F{^{1}H} NMR (CH$_2$Cl$_2$): δ −125.21 (d, $^1J_{F-P}$ = 937.6 Hz). ^{31}P{^{1}H} NMR (CH$_2$Cl$_2$): δ 242.5 (d, $^1J_{P-F}$ = 937.6 Hz). IR (ν(CO), CH$_2$Cl$_2$ solution): 1936 cm^{-1}.

X-ray Structure Analyses of 6 and 8a. Crystallographic and experimental details of X-ray crystal structure analyses are given in Table 1. Suitable crystals of **6** and **8a** were mounted independently on an Enraf-Nonuis CAD-4 automatic diffractometer. Data were collected at room temperature. Intensities were corrected for Lorentz and polarization effects in the usual manner. The structures were solved by a combination of direct methods[31] and Fourier synthesis[32] and refined by full-matrix least-squares calculations. All non-hydrogen atoms were refined anisotropically, and hydrogen atoms were treated isotropically. Final values of R = 0.054 and R_w = 0.051 for compound **6** and R = 0.049 and R_w = 0.047

for compound **8a** were obtained (R_w = [$\sum w||F_o| - |F_c||^2/\sum w|F_o|^2]^{1/2}$ and $w = 4F_o^2/\sigma^2(F_o)$). All calculations were performed using teXsan[33] with neutral atom scattering factors from Cromer and Waber,[34] Δf and $\Delta f''$ values,[35] and mass attenuation coefficients.[36] Anomalous dispersion coefficients were included in F_c.

Supporting Information Available: Full listings of atomic coordinates, anisotropic thermal parameters, bond lengths, and bond angles for **6** and **8a** (11 pages). This material is contained in many libraries on microfiche, immediately follows this article in the microfilm version of the journal, can be ordered from the ACS, and can be downloaded from the Internet; see any current masthead page for ordering information and Internet access instructions.

OM9507585

(31) SAPI91: Fan, H.-F. Structure Analysis Programs with Intelligent Control; Rigaku Corp., Tokyo, Japan, 1991.
(32) DIRDIF92: Beurskens, P. T.; Admiraal, G.; Beurskens, G.; Bosman, W. P.; Garcia-Granda, S.; Gould, R. O.; Smits, J. M. M.; Smykalla, C. The DIRDIF Program System, Technical Report of the Crystallography Laboratory; University of Nijmegen, Nijmegen, The Netherlands, 1992.
(33) teXsan: Crystal Structure Analysis Package; Molecular Structure Corp. The Woodlands, TX, 1985, 1992.
(34) Cromer, D. T.; Waber, J. T. *International Tables for X-ray Crystallography*; Kynoch Press: Birmingham, England, 1974; Vol. IV, Table 2.2 A.
(35) Creagh, D. C.; McAuley, W. J. In *International Tables for Crystallography*; Wilson, A. J. C., Ed.; Kluwer Academic: Boston, 1992; Vol C, Table 4.2.6.8, pp 219−222.
(36) Creagh, D. C.; Hubbell, J. H. *International Tables for Crystallography*; Wilson, A. J. C., Ed.; Kluwer Academic: Boston, 1992; Vol C, Table 4.2.4.3, pp 200−206.